Chemistry–A European Journal
Research Article
doi.org/10.1002/chem.202200121
Chemistry Europe
European Chemical Societies Publishing
www.chemeurj.org

Ligand-Induced Donor State Destabilisation – A New Route to Panchromatically Absorbing Cu(I) Complexes

Jens H. Tran,[a] Philipp Traber,[a] Bianca Seidler,[a] Helmar Görls,[b] Stefanie Gräfe,[a, c] and Martin Schulz*[a, d]

Abstract: The intense absorption of light to covering a large part of the visible spectrum is highly desirable for solar energy conversion schemes. To this end, we have developed novel anionic bis(4*H*-imidazolato)Cu(I) complexes (cuprates), which feature intense, panchromatic light absorption properties throughout the visible spectrum and into the NIR region with extinction coefficients up to 28,000 $M^{-1}cm^{-1}$. Steady-state absorption, (spectro)electrochemical and theoretical investigations reveal low energy (Vis to NIR) metal-to-ligand charge-transfer absorption bands, which are a consequence of destabilized copper-based donor states. These high-lying copper-based states are induced by the σ-donation of the chelating anionic ligands, which also feature low energy acceptor states. The optical properties are reflected in very low, copper-based oxidation potentials and three ligand-based reduction events. These electronic features reveal a new route to panchromatically absorbing Cu(I) complexes.

Introduction

Photoactive Cu(I) complexes have developed as an important alternative to rare metal-based complexes (e.g. Ru(II), Ir(III) or Pt(II)) for applications as photosensitizers in solar energy conversion schemes or photocatalysis.[1,2,11,3–10] Typically, bis(diimine) complexes with phenanthroline-type or bipyridine-type ligands are used, which feature strong absorption in the UV part but moderate absorption in the visible part of the spectrum.[1,10] Metal-to-ligand charge-transfer transitions (MLCT), which are important for light-driven electron-transfer processes, are usually observed in the visible range.[1,10] In order to harvest a large part of the UV-Vis-NIR spectrum, for example for solar energy conversion,[7,12] photocatalytic transformations[4] or to avail the diagnostic window for medical and diagnostic applications,[13–15] it is highly desirable to enhance the intensity of MLCT absorptions and to broaden the absorption towards the NIR region. This can be achieved by the destabilization of the metal-centred donor state and the stabilization of the ligand-based acceptor state. For Cu(I) complexes, the stabilization of the acceptor states is a widely employed approach, often focused on the extension of the diimine ligand's π-system.[7,11,16–20] For instance, 4,7-di(phenylethynyl)-substituted phenanthroline Cu(I) complexes[17,20] were found to absorb an appreciable amount of light throughout the visible range peaking around 490 nm ($\varepsilon = 16{,}000\ Lmol^{-1}cm^{-1}$). The extended phenylethynyl π-system allowed for long wavelength absorption without steric deterioration. A further improvement was achieved with $[Cu(I)(bis\text{-}(aryl)acenaphthenequinonediimine)_2]^+$ complexes, which show strong MLCT bands peaking at 580 nm ($\varepsilon = 20{,}000\ Lmol^{-1}cm^{-1}$).[21,22] Here the low energy acenaphthene acceptor orbitals promote a considerable red shift of the MLCT bands with respect to $[Cu(I)(diimine)_2]^+$ complexes. Furthermore, donor-acceptor complexes[23] were designed, to achieve the destabilization of the donor state and the stabilization of the acceptor state, such as heteroleptic diimine complexes.[7,11,24–26] However, for complexes with extended π-systems the absorption properties may be governed by ligand-based processes. Destabilisation/stabilisation of the donor/acceptor states was demonstrated with heteroleptic Cu(I) complexes, which feature strong σ-donating carbene ligands.[27,28]

For homoleptic Cu(I) complexes, the concept of a destabilisation of the copper-based donor states and stabilization of the ligand-based acceptor states has not been exploited as of yet. But this is of great interest as it conceptually allows to tune MLCT transitions along a broader range of the electromagnetic spectrum.

[a] *J. H. Tran, P. Traber, B. Seidler, Prof. Dr. S. Gräfe, Dr. M. Schulz*
Institute of Physical Chemistry
Friedrich Schiller University Jena
Helmholtzweg 4, 07743 Jena (Germany)
E-mail: martin.schulz.1@uni-jena.de

[b] *Dr. H. Görls*
Institute of Inorganic and Analytical Chemistry
Friedrich Schiller University Jena
Humboldtstr. 8, 07743 Jena (Germany)

[c] *Prof. Dr. S. Gräfe*
Fraunhofer Institute for Applied Optics and Precision Engineering (Fraunhofer IOF)
Albert-Einstein-Str.7, 07745 Jena (Germany)

[d] *Dr. M. Schulz*
Department Functional Interfaces
Leibniz Institute of Photonic Technology Jena (Leibniz-IPHT)
Albert-Einstein-Str. 9, 07745 Jena (Germany)

Supporting information for this article is available on the WWW under https://doi.org/10.1002/chem.202200121

In this contribution, we investigate a series of anionic bis(4*H*-imidazolato)Cu(I) complexes (cuprates **1**–**5**, Scheme 1), where the two chelating, anionic 4*H*-imidazolate ligands destabilize the copper-based donor states while stabilizing the ligand-based acceptor-states. This behaviour is the consequence of the interaction of the Cu(I) centre with the ligand chromophore, which represents an oxonole-type pentamethine.[29–31] As a result, extraordinary broad and intense absorption bands are observed that are composed of ligand-centred (LC) and intense, low energy MLCT transitions, spanning the visible and NIR range, well beyond 700 nm.

Results and Discussion

Synthesis

The title bis(4*H*-imidazolato)Cu(I) complexes (**1**–**5**) were synthesized by addition of $[Cu(I)(acetonitrilo)_4]PF_6$ to the deprotonated 4*H*-imidazole ligand (HIm). The 4*H*-imidazole ligand was deprotonated by the weakly basic anion exchange resin Amberlyst A21 as solid phase base (Scheme 1). Homogeneous approaches using amine bases, such as triethylamine, diisopropylethylamine or 1,8-diaza-bicyclo [5.4.0]undec-7-en (DBU) proved to be unsuccessful due to decomplexation during the workup procedure. Upon deprotonation of the 4*H*-imidazole ligands with Amberlyst A21 in acetonitrile the obtained 4*H*-imidazolates (Im^-) bind to the Amberlyst A21 beads, leading to a colour change from white (pristine beads) to bright red. Subsequent addition of $[Cu(I)(acetonitrilo)_4]PF_6$ changes the colour of the beads to dark blue, which indicates the formation of the cuprate. The beads were separated from the solution by filtration, washed with acetonitrile and dried. During this process, the anionic cuprates are retained on the beads.

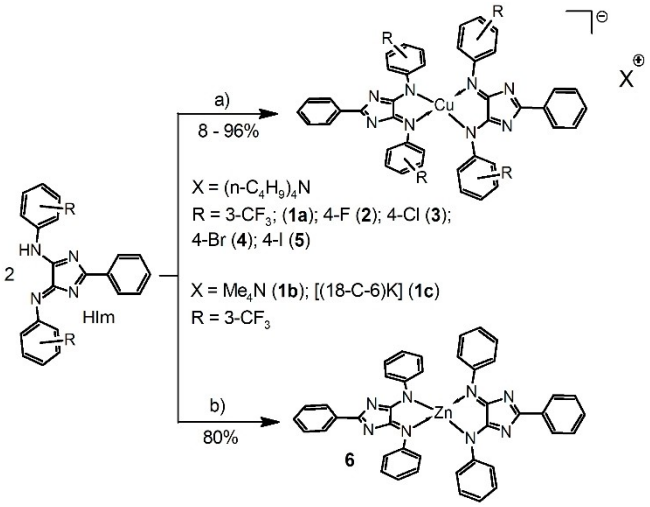

Scheme 1. General reaction scheme towards the anionic Cu(I) complexes **1**–**5** and the neutral Zn(II) complex **6**: a) Deprotonation on the anion exchange resin Amberlyst A21 and exchange with TBAF•3 H_2O (**1 a** and **2**–**5**), NMe_4Cl (**1 b**) or [K(18-crown-6)]F (**1 c**). b) The neutral Zn(II) complex **6** was obtained by reaction with diethylzinc.[32]

The cuprates were removed from the beads via anion exchange with a 1.2-fold excess of 1 M tetrabutylammonium fluoride/THF solution. The observed decolourization of the beads indicates the exchange of cuprate ions by fluoride ions and the obtained dark blue solution was separated from the beads by filtration. Further anion exchange experiments with tetrabutylammonium chloride (TBACl), tetramethylammonium chloride or tetraoctyl bromide revealed that fluoride shows the highest exchange performance as deduced by in situ ^{1}H NMR experiments (for these experiments, the resulting complexes were not isolated). The exchange performance was quantified as the ratio between tetraalkyl-ammonium ions and cuprate ions in the solution after anion exchange. The obtained crude product was further purified by a short column on basic alumina to remove excess TBAF and $TBAPF_6$, which was also separated from the beads as identified by ^{31}P and ^{19}F NMR spectroscopy. The identity and purity of the obtained complexes was confirmed by NMR spectroscopy, mass spectrometry and elemental analysis as well as by single crystal X-ray diffraction (see below). All cuprates reported in this work are stable as solids under atmospheric conditions as well as in a range of organic solvents including toluene, dichloromethane, tetrahydrofuran or acetonitrile. However, decomplexation was observed in the presence of weak acids, such as acetic acid.

The application of Amberlyst A21 not only greatly facilitates the workup procedure and prevents decomplexation, but the route via heterogeneous deprotonation allows to synthesize the title cuprates with different counter cations. This was exemplary shown with tetramethylammonium (**1 b**) and potassium 18-crown-6 (**1 c**) cuprates in the present work. Noteworthy, attempts to obtain cuprates with phenyl or toly *N*-aryl moieties (R=H, CH_3; cf. Scheme 1) were not successful due to decomplexation during the work-up procedure. Indications for the formation of the respective cuprates were found in ^{1}H NMR spectra of the reaction solutions. The Zn(II) complex **6** was prepared as a reference compound according to literature[32] (see Scheme 1), since metal-centred redox events are absent in Zn(II) complexes.

Structural Characterization

The structure of cuprates in solutions as well as in the solid state was investigated by one- and two-dimensional NMR spectroscopy, mass spectrometry, elemental analysis, and single crystal X-ray diffraction. NMR spectroscopy revealed that the obtained complexes are highly symmetric, as only one set of NMR signals was observed for both ligands. This means that both, the *N*-aryl and 2-aryl rings are indistinguishable, and one set of signals was obtained for the two 2-aryl and the four *N*-aryl moieties, respectively. The presence of two ligands was confirmed by the observation of the respective molecule peak with ESI-MS (assigned by the isotope pattern) as well as by elemental analysis and X-ray diffraction (see below). In addition, the NMR spectra indicated conformational flexibility of the *N*-aryl and 2-aryl moieties. The signals of the tetrabutylammonium counter ion were also present in the proton and carbon NMR

spectra and a comparison of the ^{1}H NMR integrals confirmed a 1:1 ratio between the cuprate and the tetrabutylammonium ion. ^{19}F and ^{31}P NMR spectroscopy confirmed the absence of F^- and PF_6^-.

The solid-state structure of Cu(I) complexes gives insights into the ground state electronics and steric effects. Single crystals, suitable for X-ray diffraction could be obtained from the cuprates **1a**, **1c**, **2** and **3**, by slow vapor diffusion from mixtures of dichloromethane or ethyl acetate with toluene or heptane. The molecular structure of **2** is exemplarily shown in Figure 1. In all structures, Cu(I) is found in a distorted tetrahedral coordination environment with dihedral angles given by both N–Cu–N planes of 65.3° (**1a**), 79.6° (**1c**), 86.3° (**2**) and 85.3° (**3**). The smaller dihedral angles found for **1a** and **1c** are attributed to packing effects, imposed through interactions of the fluorine atoms with protons of the tetrabutylammonium or $[K(18C6)]^+$ counter ions. Furthermore, dispersive interactions of adjacent molecules between the 2-aryl rings (**1**, average distance ca. 3.3 Å) are found.

Similar N–Cu–N bite angles as well as comparable Cu–N bonds length were found for all four complexes **1a**, **1c**, **2** and **3** (see Table S1 and Figures S32–S34) and are in the expected range (e.g. as found for bisphenanthroline-type complexes).[33–36] However, the Cu–N bonds of the cuprates are about 0.13 Å shorter, than in the respective [Cu(I)(xantphos)(4*H*-imidazolato)] complexes.[37] This observation is in agreement with reports on Cu(I)-phenanthroline complexes[19,38,39] where similar bond length differences of about 0.1 Å were observed. These differences mainly attributed to the steric bulk of the xantphos ligand. The ligands are not symmetry equivalent in the solid-state, but bite angles are almost identical within one complex. C–N and C–C bond lengths and angles are in the expected range.[35,36] Despite the coplanarity of the 2-aryl ring with the 4*H*-imidazole core, as found in the solid state, the connecting C–C bonds have single bond character. Also, for the complexes **2** and **3** both *N*-aryl rings were found coplanarily arranged with respect to the 4*H*-imidazole core, which is attributed to the packing. Note that the NMR data in solution indicates free rotation of the *N*-aryl rings at room temperature (see above).

Ground-state absorption properties of the reported complexes follow a general trend for homoleptic Cu(I) complexes to be red shifted with respect to the xantphos (or related) heteroleptic congeners[10,11,40] and the UV-Vis-NIR spectra are presented in Figure 2. The electronic absorptions are unusually broad and span from the UV to the NIR region to about 1000 nm. All complexes show similar features and exhibit a strong absorption band in the UV region at about 290 nm (ε = 45,000–55,000 $Lmol^{-1}cm^{-1}$) and an intense double band in the visible region peaking at about 580 nm (ε = 20,000–28,000 $Lmol^{-1}cm^{-1}$). The double band is flanked by a blue shoulder at around 475 nm (ε = 12,500–20,000 $Lmol^{-1}cm^{-1}$) and a red shoulder at around 680 nm (ε = 7,500–12,000 $Lmol^{-1}cm^{-1}$). Additionally, a weaker band around 850 nm ($\varepsilon < 5000$ $Lmol^{-1}cm^{-1}$) is observed. The underlying transitions were assigned by a comparison with the parent deprotonated ligand,[30,37,41] as well as on the basis of TD-DFT calculations. For the DFT analysis, the geometry of the complexes **2**–**5** was optimized on the PBE0/def2-SV(P)[42] level of theory in an acetonitrile solvent sphere, modelled by the IEF-PCM formalism:[43–46] the optimized geometries are in good agreement with X-ray diffraction results (see Table S1). The geometry optimization was conducted without symmetry constraints but yielded symmetrical structures and hence, the calculated MOs are symmetrically distributed over both ligands. No DFT analysis was conducted with complex **1** in this study, since the *m*CF_3 substituents require the consideration of different rotamers,[30] which was out of the scope of this study.

The optical transitions obtained by the TD-DFT calculations are qualitatively in very good agreement with the experimentally obtained data (see Figure 3 and Supporting Information for more details). Evaluation of the transition character (metal-to-ligand, MLCT or ligand-centred, LC) was achieved with the

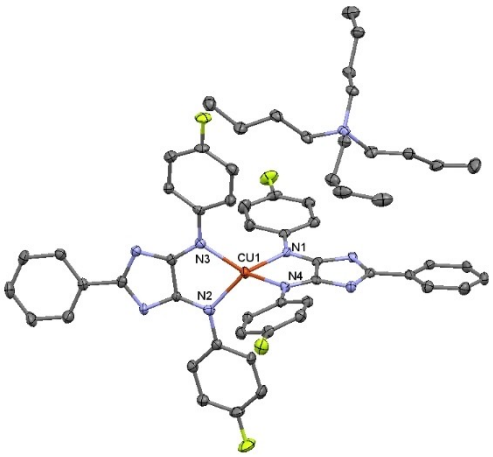

Figure 1. Molecular structure of **2** determined by single crystal X-ray diffraction. Ellipsoids are drawn at the 50% probability level. H-atoms and solvent molecules have been omitted for clarity.

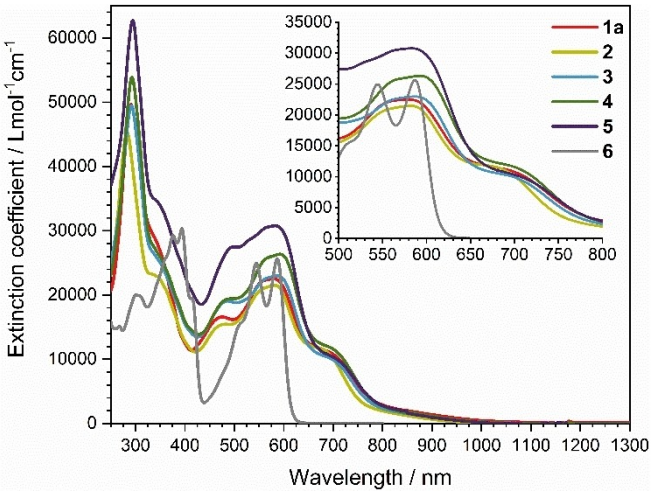

Figure 2. Absorption spectra of the Cu(I) complexes **1a**, and **2**–**5** in acetonitrile and Zn complex **6** in dichloromethane. The inset highlights the intense absorption features in the Vis and NIR spectrum.

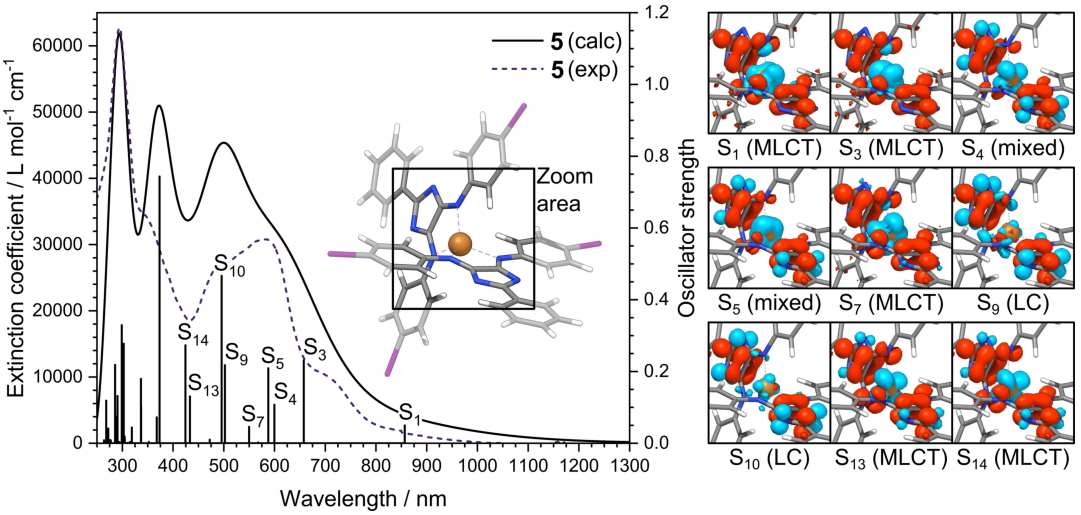

Figure 3. Comparison of the experimental and calculated electronic transitions of complex **5**. Electron density differences (electron-red; hole-blue) as well as their characters obtained by analysis with TheoDORE[47] are given for selected transitions.

TheoDORE toolbox.[47] Data evaluation revealed, that the bright lowest energy transitions (S_1 at 850 and S_3 at 660 nm) can clearly be assigned to $d_{Cu-\pi}$ MLCT transitions located on the 4*H*-imidazolate core. Furthermore, bright MLCT transitions were found at about 550 (S_7) and 430 nm (S_{13}, S_{14}). These transitions are flanked by bands with mixed metal and ligand contributions at about 590 nm (S_4 and S_5). Pure ligand-based transitions are found at 500 nm (S_9 and S_{10}) and at higher energies, i.e. in the UV part.

It is interesting to note, that throughout the NIR and visible range, only two acceptor orbitals are found, namely LUMO and LUMO + 1 (see Table S3–S10). Both acceptor orbitals are localized on the 4*H*-imidazolate core with minor contributions from the 2-aryl and *N*-aryl rings.

The band assignment is further supported by the comparison with the Zn complex **6** (see Figure S19b). The Zn complex **6**, which lacks MLCT transitions, exhibits a sharp, ligand-based double band at (544 and 587 nm), with a red shoulder around 510 nm. This band structure compares well to those of the Cu(I) complexes **1 a**, and **2**–**5**. However, the less structured shape of the Cu(I) complexes as well as additional bands on the high and low energy side of the absorption maximum suggest that MLCT transitions contribute to the absorption of the Cu(I) complexes as also found by TD-DFT (cf. Figure 3). It is important to note that the Cu(I) complexes are not emissive neither in acetonitrile nor in dichloromethane or in the solid state, from 500 to 1700 nm. The low energy absorption suggests an even lower energy gap between the lowest excited triplet state and the ground state, which would render non-radiative transitions the major deactivation pathway (energy gap law). However, the Zn complex **6** shows a structured emission, which peaks at 610 and 660 nm (see Figure S23). The small Stokes-shift and the mirror image behaviour suggest emission from a ligand-based singlet state.

Ground-state electronic properties

The ground-state electronic properties of the title complexes were investigated by NMR spectroscopy, cyclic voltammetry and UV-Vis-spectroelectrochemistry. ^{1}H NMR spectroscopy (Figure S1–S16) allows to study the shielding of the *N*-aryl and 2-aryl (*ortho*-)protons, which is a strong indicator for the electronic situation on the 4*H*-imidazolate core. To this end, a comparison of the chemical shifts of the deprotonated ligand and the cuprates provides important insights into the change of the electronic structure upon complexation. For this NMR study, the 4*H*-imidazole ligands were deprotonated with DBU in the NMR tube in CD_2Cl_2 solution. All resonances of the deprotonated 4*H*-imidazolates are upfield shifted by about 0.2 to 0.6 ppm with respect to the parent, neutral 4*H*-imidazoles, due to the delocalized negative charge on the 4*H*-imidazolate core. This contrasts with the cuprates, where the negative charges are more localised at the donor atoms. In all complexes **1 a**, and **2**–**5**, the 2-phenyl protons are only slightly influenced and show a weak downfield shift of less than 0.1 ppm of the *ortho*-protons but a comparable upfield shift of the *meta*- and *para*-protons, with respect to the parent 4*H*-imidazoles. For all *para*-substituted *N*-aryl compounds (**2**–**5**), the same pattern is found showing a downfield shift for the *N*-aryl *ortho*-protons by about 0.2 ppm and an upfield shift of the *meta*-protons of about 0.3 ppm. Complex **1 a** also shows an upfield shift of 0.3 ppm for both the *para*- and *meta*-position as well as a 0.5 ppm downfield shift for the *ortho*-proton next to the CF_3 group. The *ortho*-proton opposite to the CF_3 group is nearly unaffected. Although these changes are modest, they indicate an electronic situation with diminished electron density on the 4*H*-imidazolate core, yet an increased electron density at the periphery. These observations are in contrast to the complexation-induced upfield shifts observed for the earlier reported heteroleptic [Cu(I)(xantphos)(4*H*-imidazolato)] complexes.[37] For the heteroleptic complexes, an increased electron density on

the 4*H*-imidazolate ligand along with a decreased electron density on the xantphos ligand was observed.[36]

The lower electron density on the 4*H*-imidazole core of the complexes **1 a**, and **2**–**5** stabilizes additional charges on the 4*H*-imidazolate core, for example by ground-state reduction or light-induced charge transfer. The increased charge density on the Cu(I) centre results in MLCT transitions in the NIR range and is further reflected in low oxidation potentials between −0.08 and −0.22 V vs. Fc/Fc^+ (see below).

The ground-state redox properties were investigated to obtain further insights into the electronic and redox properties.

Cyclic voltammetry measurements were conducted at a glassy carbon working electrode against a Ag/Ag^+ pseudo reference electrode in acetonitrile and $TBAPF_6$ (0.1 M) electrolyte (Figure S24–S28). The observed potentials are reported against the Fc/Fc^+ couple and are summarized in Table 1 (the cyclic voltammograms are given in Figures S24–S28).

The cuprates show a complex redox behaviour, which is displayed by several redox events during the cathodic scan. All electrochemical reduction events are attributed to be ligand-based. This assignment is based on the comparison of the observed reduction potentials with those of the parent 4*H*-imidazoles[48–50] as well as with the earlier reported [Cu(I)(xantphos)(4*H*-imidazolato)] complexes.[31,37] All studied cuprates feature two reversible or quasi-reversible reduction waves (E^{I}_{red}, E^{II}_{red}; see Table 1), followed by an irreversible reduction wave (E^{III}_{red}). Stepwise investigation of the reduction waves showed pure electrochemical behaviour. However, when sweeping to potentials lower than the most cathodic peak, additional peaks on the backward scan occurred, which indicate subsequent chemical reactions. Additionally, all cuprates showed a reversible or quasi-reversible Cu(I)/Cu(II) oxidation wave. The latter is absent in the respective Zn(II)-complex **6**, as well as in the free ligands, which thus supports the assignment to a copper-based process. Only weak signals were obtained for **5**, which is due to the low solubility in acetonitrile, and decomposition reactions cannot be excluded. Thus, the electrochemical properties could not be assigned unambiguously.

To further understand the electronic properties of the novel cuprate, UV-Vis spectroelectrochemistry investigations were carried out and the results are depicted in Figure 4 and S29–S31. The differential absorption spectrum obtained at the first reduction wave shows positive contributions from 500 to 1100 nm, with the strongest contribution between 550–750 nm. These findings indicate that the unpaired electron of the one-electron reduced species is localised on one ligand, which leads to a positive differential absorption in a wavelength region where also the $[Cu(I)(xantphos)(4\text{-imidazolato})]^-$ radical absorbs.[31,51] This interpretation is supported by the DFT-calculated spin density (Figure S39). Absorption differences obtained at potentials below −1 V, i.e. for the two-electron-reduced cuprate show weak positive contributions above 750 nm, as well as negative contributions between 550–750 nm (Figure 4A). The loss of the typical cuprate absorption pattern and the occurrence of a broad NIR band is interpreted as the one-electron reduction of each of both ligands. This interpretation is supported by DFT calculations, which indicate a triplet biradical (Figure S39). Upon polarization at anodic potentials, negative differential absorptions are observed, which fit well to the MLCT-assigned bands of the inverted absorption spectrum, indicating the loss of these transitions in the oxidized complexes. Positive contributions around 500 nm may be assigned to Cu(II) d-d transitions (Figure 4B).[51]

For each complex, the difference between the first and the second reduction potential as well as the second and the third reduction potential lies between 250–300 mV and 300–400 mV, respectively. In particular, the large difference between the first and the second reduction potential indicates considerable

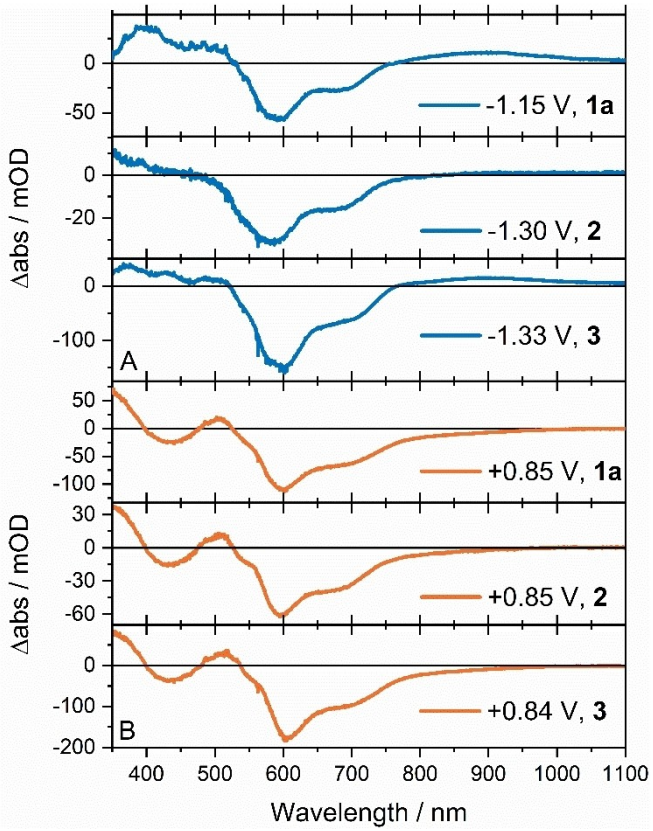

Figure 4. UV-Vis-SEC difference spectra of **1 a**, **2** and **3** for the second reduction (A, blue) at −1.15, −1.30 and −1.33 V and the oxidation (B, orange) at +0.85, +0.85 and +0.84 V, respectively. The spectra were measured in 0.1 M $TBABF_4$ as supporting electrolyte in anhydrous and degassed acetonitrile. The difference spectra were obtained by subtracting the open circuit potential (OCP) spectrum from the reduced/oxidized spectra.

Table 1. Half step potentials [V], obtained by cathodic (E_{red}) and anodic (E_{ox}) cyclic voltammetry in acetonitrile (**1 a**–**5**) and DMF (**6**) are given. All potentials are referenced vs. Fc/Fc^+.

	E^{I}_{red}	E^{II}_{red}	E^{III}_{red}	E^{IV}_{red}	E_{ox}
1 a	−1.43	−1.71	−2.02	not observ.	−0.08
2	−1.70	−1.98	−2.38	not observ.	−0.22
3	−1.59	−1.84	−2.24	not observ.	−0.17
4	−1.56	−1.83	−2.14	not observ.	−0.16
5	n.a.	n.a.	n.a.	n.a.	−0.18
6	−1.06	−1.31	−2.18	−2.42	not observ.

electronic coupling between the two ligands.[52] For the *para*-substituted cuprates **2**–**4**, the differences between the individual reduction potentials reflect the $+M$ (*p*F) as well as -*I* effect (*p*Cl, *p*Br) of the substituents, while the third reduction potentials steadily decrease from complex **2** to **4**, each by ca. 100 mV. The anodic wave, attributed to the Cu(I)/Cu(II) oxidation, is observed at very low potentials and indicates the increased electron density on the copper centre. The oxidation potential of **1 a** is about 80 mV more positive, compared to **2**–**5**. This is mainly attributed to the steric demand imposed by *meta*-substituent of **1**. This steric demand impedes the reorientation from the tetrahedral Cu(I) to the square planar Cu(II) coordination environment in the course of the oxidation and therefore shifts the oxidation potentials to more positive values. For all described complexes, the oxidation potentials are considerably lower than those of homoleptic diimine complexes, such as $[Cu(I)(phenanthroline)_2]^+$ complexes with anodic potentials of 0.1 to 0.8 V.[21,53–55] Also, the related heteroleptic [Cu(I)(xantphos)(4*H*-imidazolato)] complexes show considerably higher oxidation potentials (ca. 0.7 V).[31,37] The low oxidation potentials of the title complexes are also reflected in the low energy MLCT transitions (see below) and follow the trend that the oxidation of the homoleptic complexes are usually lower than those of the respective xantphos (or related) complexes.[6,10]

The [Zn(II)bis(4*H*-imidazolato)] complex **6** was synthesized as a reference system with a redox-silent central metal. Four reduction waves are observed for complex **6**, which are all ligand-based. This is in agreement with the two electron reductions, reported for the parent 4*H*-imidazoles[48–50] as well as for the [Cu(I)(xantphos)(4*H*-imidazolato)] complexes.[31,37] In the Zn(II) complex **6**, both ligands are similarly strong coupled (based on the half-step potential difference), but the nominal $+2$ charge of the zinc ion stabilizes four reduction steps in a comparable potential window with respect to the copper complexes. However, the Cu(I) complexes and the Zn complex have been measured in different solvents, which precludes a direct comparison.

Conclusion

We have introduced novel, anionic bis(4*H*-imidazolato)Cu(I) complexes which possess compelling light absorption properties, that span from the UV to the NIR range. These absorption properties are a consequence of the destabilization of the Cu(I)-based donor states by the chelating, anionic 4*H*-imidazolate ligands, which act as σ-donors and increase the electron density on the metal centre. This is reflected by the unusually low, copper-based oxidation potentials. Additionally, low lying acceptor states are available on the 4*H*-imidazolate ligands. Altogether, the exocyclic σ-donating nitrogen donors and the relatively small pentamethine chromophore of the ligands avails low energy MLCT transitions in the green to NIR range with high extinction coefficients as well as ligand-centred transitions in the blue part of the absorption band. This is conceptually different from approaches, which aim on the extension of the ligand π-system or ligand-based donor acceptor complexes and may contribute to the development of photoactive Cu(I) complexes. Despite the observed sensitivity of (4*H*-imidazolato)Cu(I) complexes towards acids, application scenarios under neutral or basic conditions may be envisioned. The panchromatic absorption and electrochemical properties of the described anionic bis(4*H*-imidazolato)Cu(I) complexes make them attractive candidates as photosensitizers in solar energy conversion and photoredox chemistry. The assessment of their excited-state and photosensitizing properties is part of ongoing investigations.

Supporting Information: Synthetic details, absorption spectra of the individual complexes and ligands, cyclic voltammetry data, spectroelectrochemistry data and computational details are available. Deposition Number(s) 1995045 (for **1 a**), 1995046 (for **1 c**), 1995047 (for **2**) and 1995048 (for **3**) contain(s) the supplementary crystallographic data for this paper. These data are provided free of charge by the joint Cambridge Crystallographic Data Centre and Fachinformationszentrum Karlsruhe Access Structures service.

Acknowledgements

We kindly acknowledge financial support by the Ernst-Abbe-Stiftung Jena for the ACD/Labs Spectrus processor license, that was used for NMR analysis. Support by the NMR platform at the Friedrich Schiller University Jena is gratefully acknowledged. The authors acknowledge funding by the Deutsche Forschungsgemeinschaft (DFG, German Research Foundation) – Projektnummer 364549901 – TRR 234 "CataLight". We like to thank Dr. Grace Lowe and Dr. Stephan Kupfer for fruitful discussions and Dr. Mathias Micheel for the measurement of the emission spectra. All calculations have been performed at the Universitätsrechenzentrum of the Friedrich Schiller University Jena. Open Access funding enabled and organized by Projekt DEAL.

Conflict of Interest

The authors declare no conflict of interest.

Data Availability Statement

The data that support the findings of this study are available in the supplementary material of this article.

Keywords: ab initio calculations · cuprates · electrochemistry · N ligands · UV/Vis spectroscopy

[1] V. Leandri, A. R. P. Pizzichetti, B. Xu, D. Franchi, W. Zhang, I. Benesperi, M. Freitag, L. Sun, L. Kloo, J. M. Gardner, *Inorg. Chem.* **2019**, *58*, 12167–12177.
[2] *Visible Light Photocatalysis in Organic Chemistry* (Eds. C. Stephenson, T. Yoon, D. W. C. MacMillan), Wiley-VCH Verlag GmbH & Co. KGaA, Weinheim, Germany, **2018**.

[3] O. S. Wenger, *J. Am. Chem. Soc.* **2018**, *140*, 13522–13533.
[4] B. M. Hockin, C. Li, N. Robertson, E. Zysman-Colman, *Catal. Sci. Technol.* **2019**, *9*, 889–915.
[5] A. Friedrich, O. S. Bokareva, S.-P. Luo, H. Junge, M. Beller, O. Kühn, S. Lochbrunner, *Chem. Phys.* **2018**, *515*, 557–563.
[6] D. V. Scaltrito, D. W. Thompson, J. A. O. Callaghan, G. J. Meyer, J. A. O'Callaghan, G. J. Meyer, *Coord. Chem. Rev.* **2000**, *208*, 243–266.
[7] C. E. Housecroft, E. C. Constable, *Chem. Soc. Rev.* **2015**, *44*, 8386–8398.
[8] M. Sandroni, Y. Pellegrin, F. Odobel, *Comptes Rendus Chim.* **2016**, *19*, 79–93.
[9] C. Dragonetti, M. Magni, A. Colombo, F. Fagnani, D. Roberto, F. Melchiorre, P. Biagini, S. Fantacci, *Dalton Trans.* **2019**, *48*, 9703–9711.
[10] Y. Zhang, M. Schulz, M. Wächtler, M. Karnahl, B. Dietzek, *Coord. Chem. Rev.* **2018**, *356*, 127–146.
[11] M. S. Lazorski, F. N. Castellano, *Polyhedron* **2014**, *82*, 57–70.
[12] P. D. Frischmann, K. Mahata, F. Würthner, *Chem. Soc. Rev.* **2013**, *42*, 1847–1870.
[13] J. Frangioni, *Curr. Opin. Chem. Biol.* **2003**, *7*, 626–634.
[14] K. Berg, P. K. Selbo, A. Weyergang, A. Dietze, L. Prasmickaite, A. Bonsted, B. O. Engsaeter, E. Angell-Petersen, T. Warloe, N. Frandsen, *J. Microsc.* **2005**, *218*, 133–147.
[15] M. Tim, *J. Photochem. Photobiol. B* **2015**, *150*, 2–10.
[16] C. C. Phifer, D. R. McMillin, *Inorg. Chem.* **1986**, *25*, 1329–1333.
[17] M. T. Miller, T. B. Karpishin, *Inorg. Chem.* **1999**, *38*, 5246–5249.
[18] N. Armaroli, *Chem. Soc. Rev.* **2001**, *30*, 113–124.
[19] M. Heberle, S. Tschierlei, N. Rockstroh, M. Ringenberg, W. Frey, H. Junge, M. Beller, S. Lochbrunner, M. Karnahl, *Chem. Eur. J.* **2017**, *23*, 312–319.
[20] S. Garakyaraghi, C. E. McCusker, S. Khan, P. Koutnik, A. T. Bui, F. N. Castellano, *Inorg. Chem.* **2018**, *57*, 2296–2307.
[21] P. Papanikolaou, P. D. Akrivos, A. Czapik, B. Wicher, M. Gdaniec, N. Tkachenko, *Eur. J. Inorg. Chem.* **2013**, *2013*, 2418–2431.
[22] P. A. Papanikolaou, N. V. Tkachenko, *Phys. Chem. Chem. Phys.* **2013**, *15*, 13128–13136.
[23] S. Garakyaraghi, P. Koutnik, F. N. Castellano, *Phys. Chem. Chem. Phys.* **2017**, *19*, 16662–16668.
[24] M. Sandroni, M. Kayanuma, M. Rebarz, H. Akdas-Kilig, Y. Pellegrin, E. Blart, H. Le Bozec, C. Daniel, F. Odobel, *Dalton Trans.* **2013**, *42*, 14628.
[25] M. Sandroni, L. Favereau, A. Planchat, H. Akdas-Kilig, N. Szuwarski, Y. Pellegrin, E. Blart, H. Le Bozec, M. Boujtita, F. Odobel, *J. Mater. Chem. A* **2014**, *2*, 9944–9947.
[26] R. Giereth, W. Frey, H. Junge, S. Tschierlei, M. Karnahl, *Chem. Eur. J.* **2017**, *23*, 1–7.
[27] M. Gernert, L. Balles-Wolf, F. Kerner, U. Müller, A. Schmiedel, M. Holzapfel, C. M. Marian, J. Pflaum, C. Lambert, A. Steffen, *J. Am. Chem. Soc.* **2020**, *142*, 8897–8909.
[28] B. Hupp, C. Schiller, C. Lenczyk, M. Stanoppi, K. Edkins, A. Lorbach, A. Steffen, *Inorg. Chem.* **2017**, *56*, 8996–9008.
[29] M. Schulz, C. Reichardt, C. Müller, K. R. A. Schneider, J. Holste, B. Dietzek, *Inorg. Chem.* **2017**, *56*, 12978–12986.
[30] C. Müller, M. Schulz, M. Obst, L. Zedler, S. Gräfe, S. Kupfer, B. Dietzek, *J. Phys. Chem. A* **2020**, *124*, 6607–6616.
[31] M. Schulz, N. Hagmeyer, F. Wehmeyer, G. Lowe, M. Rosenkranz, B. Seidler, A. Popov, C. Streb, J. G. Vos, B. Dietzek, *J. Am. Chem. Soc.* **2020**, *142*, 15722–15728.
[32] R. Beckert, J. Atzrodt, H. Görls, *Heterocycles* **1999**, *51*, 763.
[33] M. T. Miller, P. K. Gantzel, T. B. Karpishin, *Inorg. Chem.* **1998**, *37*, 2285–2290.
[34] M. T. Miller, P. K. Gantzel, T. B. Karpishin, *J. Am. Chem. Soc.* **1999**, *121*, 4292–4293.
[35] F. H. Allen, O. Kennard, D. G. Watson, L. Brammer, A. G. Orpen, R. Taylor, *J. Chem. Soc. Perkin Trans. 2* **1987**, 1–19.
[36] A. G. Orpen, L. Brammer, F. H. Allen, O. Kennard, D. G. Watson, R. Taylor, *J. Chem. Soc. Dalton Trans.* **1989**, S1.
[37] M. Schulz, F. Dröge, F. Herrmann-Westendorf, J. Schindler, H. Görls, M. Presselt, *Dalton Trans.* **2016**, *45*, 4835–4842.
[38] M. Rentschler, S. Iglesias, M. Schmid, C. Liu, S. Tschierlei, W. Frey, X. Zhang, M. Karnahl, D. Moonshiram, *Chem. Eur. J.* **2020**, *26*, 9527–9536.
[39] R. Giereth, I. Reim, W. Frey, H. Junge, S. Tschierlei, M. Karnahl, *Sustain. Energy Fuels* **2019**, *3*, 692–700.
[40] T. Tsukuda, A. Nakamura, T. Arai, T. Tsubomura, *Bull. Chem. Soc. Jpn.* **2006**, *79*, 288–290.
[41] J. Atzrodt, J. Brandenburg, C. Käpplinger, R. Beckert, W. Günther, H. Görls, J. Fabian, *J. Prakt. Chem.* **1997**, *339*, 729–734.
[42] C. Adamo, V. Barone, *J. Chem. Phys.* **1999**, *110*, 6158–6170.
[43] E. Cancès, B. Mennucci, J. Tomasi, *J. Chem. Phys.* **1997**, *107*, 3032–3041.
[44] B. Mennucci, E. Cances, J. Tomasi, *J. Phys. Chem. B* **1997**, *101*, 10506–10517.
[45] J. Tomasi, B. Mennucci, R. Cammi, *Chem. Rev.* **2005**, *105*, 2999–3093.
[46] E. Cancès, B. Mennucci, *J. Math. Chem.* **1998**, *23*, 309–326.
[47] F. Plasser, *J. Chem. Phys.* **2020**, *152*, 084108.
[48] T. Gebauer, R. Beckert, D. Weiß, K. Knop, C. Käpplinger, H. Görls, *Chem. Commun.* **2004**, *0*, 1860–1861.
[49] R. Beckert, C. Hippius, T. Gebauer, F. Stöckner, C. Lüdigk, D. Weiß, D. Raabe, W. Günther, H. Görls, *Z. Naturforsch. B* **2006**, *61*, 437–447.
[50] M. Matschke, R. Beckert, *Molecules* **2007**, *12*, 723–734.
[51] B. Seidler, M. Sittig, C. Zens, J. H. Tran, C. Müller, Y. Zhang, K. R. A. Schneider, H. Görls, A. Schubert, S. Gräfe, *J. Phys. Chem. B* **2021**, *125*, 11498–11511.
[52] J. Hankache, O. S. Wenger, *Chem. Rev.* **2011**, *111*, 5138–5178.
[53] M. K. Eggleston, D. R. McMillin, K. S. Koenig, A. J. Pallenberg, K. Eggleston, D. R. McMillin, K. S. Koenig, A. J. Pallenberg, P. Corporation, A. Ne, *Inorg. Chem.* **1997**, *1669*, 2435–2439.
[54] Y. Zhang, M. Heberle, M. Wächtler, M. Karnahl, B. Dietzek, M. Waechtler, M. Karnahl, B. Dietzek, *RSC Adv.* **2016**, *6*, 105801–105805.
[55] T. P. Nicholls, C. Caporale, M. Massi, M. G. Gardiner, A. C. Bissember, *Dalton Trans.* **2019**, *48*, 7290–7301.

Manuscript received: January 13, 2022
Accepted manuscript online: March 9, 2022
Version of record online: March 25, 2022